Conf-941203--13

SAND94-1597C

# GaAsSb-BASED HETEROJUNCTION TUNNEL DIODES FOR TANDEM SOLAR CELL INTERCONNECTS

John C. Zolper, John F. Klem, Thomas A. Plut, and Chris P. Tigges
Sandia National Laboratories, Albuquerque, NM 87185-0603

### Abstract:

We report a new approach to tunnel junctions that employs a pseudomorphic GaAsSb layer to obtain a band alignment at a InGaAs or InAlAs p-n junction favorable for forward bias tunneling. Since the majority of the band offset between GaAsSb and InGaAs or InAlAs is in the valence band, when an GaAsSb layer is placed at an InGaAs or InAlAs p-n junction the tunneling distance is reduced and the tunneling current is increased. For all doping levels studied, the presence of the GaAsSb-layer enhanced the forward tunneling characteristics. In fact, in a InGaAs/GaAsSb tunnel diode a peak tunneling current sufficient for a 1000 sun intercell interconnect was achieved with $p = 1.5\times10^{18}$ $cm^{-3}$ while a similarly doped all-InGaAs diode was rectifying. This approach affords a new degree of freedom in designing tunnel junctions for tandem solar cell interconnects. Previously only doping levels could be varied to control the tunneling properties. Our approach relaxes the doping requirements by employing a GaAsSb-based heterojunction.

### Introduction:

Tandem junction solar cells offer higher energy conversion efficiencies than single junction solar cells. Although impressive tandem solar cell performance has been demonstrated with hybrid, mechanically stacked, four-terminal tandem solar cells,[1] the full potential of monolithic, two-terminal, tandem solar cell structures has not been realized.[2] In general, a two-terminal design is preferred to reduce processing costs and to improve overall system performance. The primary obstacle to realizing high performance, two-terminal, tandem solar cells is the intercell interconnect. One solution to this problem is to make this intercell junction a tunnel junction.

Homojunction (GaAs/GaAs[3] and InGaAs/InGaAs[4,5] and heterojunction (GaAs/InGaAs,[6] AlGaAs/GaAs[7] and AlGaAs/GaInP[8]) tunnel junctions have been investigated for the intercell interconnect in tandem solar cells. Representative tunnel diode results are summarized in Table I and compared to our results reported here. For forward bias tunneling to occur there must be empty valence band states at the same energy level as full conduction band states and the distance between these states must be on the order of 100 Å. Prior to this work, this required degenerate doping on both sides of the junction with an abrupt doping profile. In practice, it is difficult to maintain the abrupt doping profile due to diffusion of the p-type dopant that smears the junction and reduces or eliminates forward bias tunneling.

Table I
Summary of previous tunnel diode approaches and results from this work.

| material system | $J_p$ ($A/cm^2$) | $V_p/J_p$ ($\Omega$-$cm^2$) | reference |
|---|---|---|---|
| GaAs/GaAs | 45 | $2\times10^{-3}$ | Basmaji[3] |
| InGaAs/InGaAs | 48 | $8.9\times10^{-4}$ | Wanlass[4] |
| InGaAs/InGaAs | 1015 | $2.5e10^{-4}$ | Medelci[5] |
| GaAs/InGaAs | 1300 | $6.2\times10^{-5}$ | Richard[6] |
| AlGaAs/GaAs | 300 | $1.7\times10^{-4}$ | Miller[7] |
| AlGaAs/GaInP | 90 | $1.7\times10^{-3}$ | Jung[8] |
| InGaAs/GaAsSb | 19904 | $5.0\times10^{-5}$ | this work |
| InAlAs/GaAsSb | 139 | $1.2\times10^{-3}$ | this work |

We report a new approach to tunnel junctions which employs a pseudomorphic GaAsSb layer to obtain a favorable band alignment at the p-n junction. The properties of InGaAs/InGaAs and InAlAs/InAlAs tunnel diodes lattice matched to InP fabricated with and without a thin $p^+$-$GaAs_xSb_{1-x}$ layer at the junction were investigated. Since the majority of the band offset between GaAsSb and InGaAs or InAlAs is in the valence band, when an GaAsSb layer is placed at an InGaAs or InAlAs p-n junction, the tunneling distance is reduced and the tunneling current is increased. This reduction in tunneling distance is evident in the energy band diagrams, calculated from the non-linear one dimensional Poison's equation, of Figs. 1 and 2.

Fig. 1(a) and 2(a) are the energy band diagrams for InGaAs and InAlAs the tunnel diodes, respectively, without the $GaAs_{0.35}Sb_{0.65}$ layer while Fig. 2(b) and 2(b) are the diodes with a 150 Å pseudomorphic p-type $GaAs_{0.35}Sb_{0.65}$ layer placed at the junction and doped at the sample level as the p-InGaAs ($5\times10^{18}$ $cm^{-3}$) or p-InAlAs ($4\times10^{19}$ $cm^{-3}$), respectively. Due to the band alignment between GaAsSb and either InGaAs or InAlAs the maximum tunneling distance across the junction is appreciably reduced when the GaAsSb layer is present. Since tunneling depends exponentially on the tunneling distance, any reduction in the tunneling distance will significantly increase the tunneling probability and thus the tunneling current. This is clearly demonstrated by the experimental results in the next section.

A primary advantage of incorporating a GaAsSb layer at the junction is that the doping requirement for the p-type side of the junction can be reduced while maintaining the same tunneling current. The reduction in p-type doping should significantly reduce dopant diffusion during growth, thus maintaining the sharp junction profile required for optimum tunneling and enhancing the overall manufacturability of two-terminal tandem solar cells.

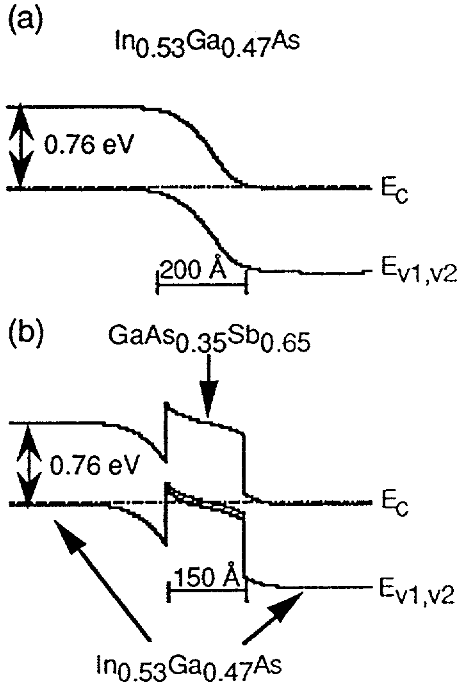


Fig. 1: Energy band diagrams for a $p^+/n^+$ InGaAs tunnel diode (a) without and (b) with a 150 Å pseudomorphic $p^+$-$GaAs_{0.35}Sb_{0.65}$ tunneling enhancement layer. $p = 5x10^{18}$ $cm^{-3}$ and $n = 1x10^{19}$ $cm^{-3}$.

### Experimental Approach:

Samples were grown on (100) $n^+$-InP substrates in a Varian Gen II molecular beam epitaxial reactor as discussed in detail in ref. 9. The epitaxial layers were nominally latticed matched to the InP substrate with the exception of the pseudomorphic GaAsSb layer. The n-type doping species was Si and p-type species was Be. Circular diodes with varied diameters were defined by a wet mesa etch down past the p/n junction. Ohmic contacts were evaporated Au/Be (p-type) and Au/Ge (n-type).

Diodes structures based on InGaAs and InAlAs were compared with and without the incorporation of the pseudomorphic GaAsSb layer. With the n-type doping concentration held constant at $1x10^{19}$ $cm^{-3}$, the effect of reducing the p-type doping from a maximum of $4x10^{19}$ $cm^{-3}$ down to 8 or $1.5x10^{18}$ $cm^{-3}$ for InGaAs-based diodes and down to $5x10^{18}$ $cm^{-3}$ for InAlAs-based diodes was studied. DC testing was done in the dark using with common current and voltage probes. Such a two probe measurement will add a series resistance to the diode measurement that will increase the measured diode specific resistivity and the peak tunneling voltage ($V_p$). Therefore, the diode resistivities reported here should be considered as an upper limit. Four terminal testing that will allow the true diode resistivity to be determined will be reported at a later date.

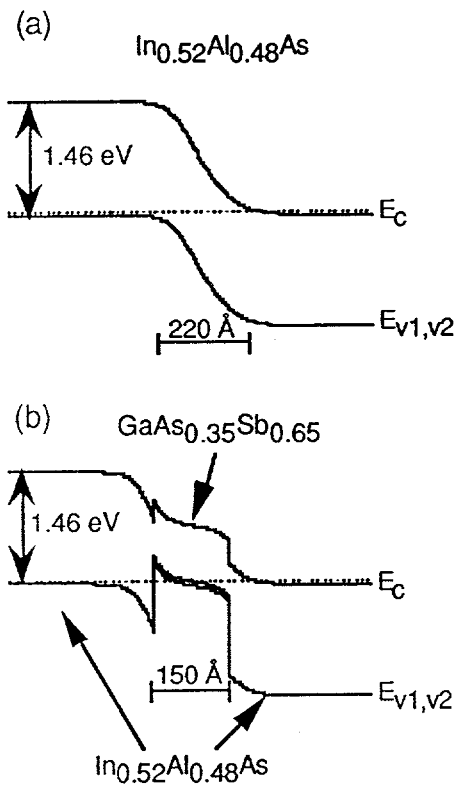


Fig. 2: Energy band diagrams for a $p^+/n^+$ InAlAs tunnel diode (a) without and (b) with a 150 Å pseudomorphic $p^+$-$GaAs_{0.35}Sb_{0.65}$ tunneling enhancement layer. $p = 4x10^{19}$ $cm^{-3}$ and $n = 1x10^{19}$ $cm^{-3}$.

### Tunnel Diode Results:

Figures 3 and 4 are scanned images of the measured two-probe forward current-voltage characteristics taken on a Tektronic's 576 curve tracer of the tunnel diode structures summarized in Tables II and III. The diodes reported had a 40 µm diameter. The thickness of the GaAsSb layer was 150 Å. Each figure includes a diode I/V characteristic, at the specified p-type doping level, both with and without the GaAsSb layer. In all cases the presence of the GaAsSb-layer enhanced the forward tunneling characteristics. For example, in the most lightly doped InGaAs diode (sample E, $p = 1.5x10^{18}$ $cm^{-3}$) with the GaAsSb-layer the peak tunneling current and

diode resistivity is still sufficient to carry the current in an InP/InGaAs tandem solar cell at 1000 suns concentration,[2,4] while the InGaAs-only diode (sample F) is rectifying. For the InAlAs diodes, which have the advantage of less absorption in the tunnel junction region compared to InGaAs diodes due to their higher bandgap ($E_g$ = 1.46 eV), the addition of the GaAsSb layer converted the diodes from rectifying to tunneling for both doping concentrations. Here again, $J_p$ on the more highly doped InAlAs/GaAsSb diode (sample H) is sufficient for the intercell interconnect of a 1000 sun InP/InGaAs tandem solar cell.

Table II

Summary of InGaAs/GaAsSb/InGaAs tunnel diode structures with and without a GaAsSb layer (150 Å) and with three p-type doping levels. The GaAsSb layers are doped p-type to the same level as the $p^+$-InGaAs. n = $1\times10^{19}$ $cm^{-3}$ for all diodes.

| ID | $p^+$-InGaAs doping (Be) $cm^{-3}$ | GaAsSb %GaSb | $J_p$ ($A/cm^2$) | $V_p/J_p$ ($\Omega$-$cm^2$) |
|---|---|---|---|---|
| A | $4\times10^{19}$ | --- | 2388 | $8.4\times10^{-5}$ |
| B | $4\times10^{19}$ | 49 | 9156 | $6.8\times10^{-5}$ |
| C | $4\times10^{19}$ | 62 | 19904 | $5.0\times10^{-5}$ |
| D | $8\times10^{18}$ | 65 | 5732 | $7.7\times10^{-5}$ |
| E | $1.5\times10^{18}$ a,b | 65 | 239 | $6.3\times10^{-4}$ |
| F | $1.5\times10^{18}$ | --- | c | c |
| G | $8\times10^{18}$ | -- | c | c |

[a] Also included a 1000 Å, $8\times10^{18}$ $cm^{-3}$ p-InGaAs contact layer

[b] Also included a 50 Å p-InGaAs ($1.5\times10^{18}$ $cm^{-3}$) spacer at the n-InGaAs interface.

[c] Samples were rectifying.

Table III

Summary of InAlAs/GaAsSb/InAlAs tunnel diode structures with and without the GaAsSb layer (150 Å) and with two p-type doping levels. The GaAsSb layers are doped p-type to the same level as the $p^+$-InAlAs.[a] n = $1\times10^{19}$ $cm^{-3}$ for all diodes.

| ID | $p^+$-InAlAs doping (Be) ($cm^{-3}$) | GaAsSb %GaSb | $J_p$ ($A/cm^2$) | $V_p/J_p$ ($\Omega$-$cm^2$) |
|---|---|---|---|---|
| H | $4\times10^{19}$ | 65 | 139 | $1.2\times10^{-3}$ |
| I | $5\times10^{18}$ b | 65 | 3.6 | $1.4\times10^{-2}$ |
| J | $4\times10^{19}$ | --- | c | c |
| K | $5\times10^{18}$ | --- | c | c |

[a] All diodes included a 500 Å $p^+$-InGaAs ($4\times10^{19}$ $cm^{-3}$) contact layer.

[b] Also included a 50 Å p-InAlAs ($5\times10^{18}$ $cm^{-3}$) spacer at the n-InAlAs interface.

[c] Samples were rectifying.

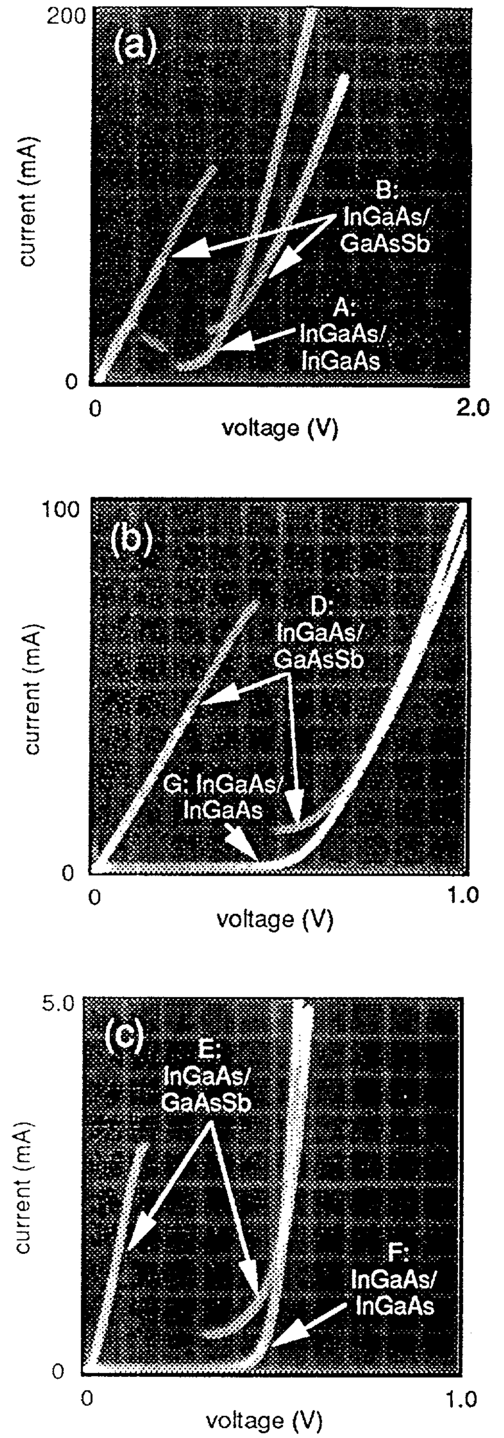


Fig. 3: InGaAs-based tunnel diodes with (a) p = $4\times10^{19}$ $cm^{-3}$, (b) p = $8\times10^{18}$ $cm^{-3}$, and (c) p = $1.5\times10^{18}$ $cm^{-3}$ with (samples B, D, and E) and without (samples A, G, and F) the GaAsSb tunneling enhancement layer. n = $1\times10^{19}$ $cm^{-3}$ for all diodes.

applicability to GaAs based tandem solar cell structures such as AlGaAs/GaAs and $GaInP_2$/GaAs.

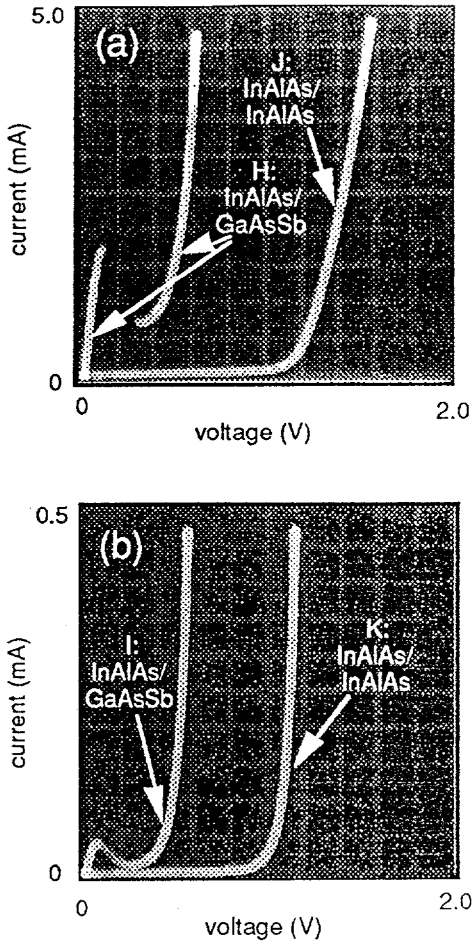


Fig. 4: InAlAs-based tunnel diodes with (a) $p = 4x10^{19}$ $cm^{-3}$ and (b) $p = 5x10^{18}$ $cm^{-3}$ with (samples H and I) and without (samples J and K) the GaAsSb tunneling enhancement layer. $n = 1x10^{19}$ $cm^{-3}$ for all diodes.

## Conclusion:

The incorporation of a pseudomorphic GaAsSb layer in a tunnel diode structure affords a new degree of freedom in designing tunnel junctions for tandem solar cell interconnects. Previously only doping levels could be varied to control the tunneling properties. In this work, we demonstrate a novel heterojunction tunnel diode design that greatly relaxes the doping requirements for tunneling. For example, InGaAs-based tunnel diodes with p as low as $1.5x10^{18}$ $cm^{-3}$ still demonstrated peak tunneling currents sufficient for use as an InP/InGaAs intercell interconnect operating at 1000 suns concentration. Future work will include applying this approach to InP/InGaAs and InAlAs/InGaAs tandem solar cells and investigating the

## Acknowledgments:


This work was performed at Sandia National Laboratories and supported by the Department of Energy under contract No. DE-AC04-94AL85000.


References:


1 L. M. Fraas, J. E. Avery, J. Martin, V. S. Sundaram, G. Girard, V. T. Dinh, T. M. Davenport, J. W. Yerkes, and M. J. O'Neill, IEEE Trans. Elec. Dev., vol. 37 pp. 443-449 (1990).

2 M. W. Wanless, T. J. Coutts, J. S. Ward, K. A. Emery, T. A. Gessert, and C. R. Osterwald, Proc. 22nd IEEE Photovoltaic Specialists Conference, pp. 38-45 (1991).

3 P. Basmaji, M. Guittard, A. Rudra, J. F. Carlin, and P. Gibart, J. Appl. Phys., 62, 2103 (1987).

4 M. W. Wanlass, J. S. Ward, K. A. Emery, and T. J. Coutts, Proc. 23rd IEEE Photovoltaic Specialists Conference, pp. 621-627, 1993.

5 N. Medelci, A. Bensaoula, M. F. Vilela, and A. Freundlich, MRS Symp. Proc., vol. 300, pp. 453-457 (1993)

6 T. A. Richard, E. I. Chen, A. R. Sugg, G. E. Höfler, and N. Holonyak, Jr., Appl. Phys. Lett., 26, pp. 3613-3615 (1993).

7 D. L. Miller, S. W. Zehr, and J. S. Harris, Jr., J. of Appl. Phys., vol 53, pp. 744-748, 1982.

8 D. Jung, C. A. Parker, J. Ramdani, ans S. M. Bedair, J. of Appl. Phys., vol 74, pp. 2090-2093, 1993.

9 J. F. Klem and S. R. Kurtz, J. Cryst. Growth, vol. 111, pp. 628-632 (1991).